Deep tissue optoacoustic imaging of polarized structures

Daniel Razansky[1,*], Claudio Vinegoni[2], and Vasilis Ntziachristos[1]

[1]Institute for Biological and Medical Imaging, Technical University of Munich and Helmholtz Center Munich, Ingolstädter Landstraße 1, 85764 Neuherberg, Germany.
[2]Center for Systems Biology, Massachusetts General Hospital and Harvard Medical School, 185 Cambridge Street, Boston, MA, 02114, USA.

ABSTRACT

The ability to image polarization-selective tissue structures may provide valuable information on tissue anatomy, morphogenesis, and disease progression. So far, intensive light scattering in biological medium has limited implementation of polarization imaging to superficial tissue layers. We suggest overcoming the scattering problem using polarization-sensitive optoacoustic imaging. Due to intrinsically high spatial resolution and sensitivity of the method, it holds promise of becoming highly accurate modality for interrogation of small polarized structures deep in biological tissues. We show initial tomographic results in tissue-mimicking phantoms having polarization dichroism contrast.

I. INTRODUCTION

Optoacoustic tomography has recently drawn much attention due to its ability to achieve optical contrast with high spatial resolution deep within diffusive biological samples [1-6]. There has been now a great interest in the development of different contrast agents and contrast mechanisms that could be appropriate for achieving molecular contrast based on optoacoustics [5,6].

We look into polarization as a possible contrast mechanism for optoacoustic imaging deep in diffusive media with tissue-like optical properties. Polarization imaging of optically diffusive media is gaining much interest due to possibility of increasing contrast of superficial tissue structures by rejecting multiple scattered photons coming from deep layers of tissue. Another important motivation is the ability to obtain contrast from certain tissue structures not distinguishable by any other mechanism. Polarization contrast has been associated with anisotropic tissue properties relating to structural elements associated with development and function, e.g. muscle cell orientation [7], birefringence of cytoskeletal filaments [8] or disease, e.g. in Alzheimer-associated amyloid-β plaque deposits [9].

However, imaging polarized structures in turbid tissues turns challenging. This is due to the fact that, during propagation in a diffusive medium, polarized light is found to rapidly lose its propagation direction and its polarization properties [10,11] due to multiple scattering events that arise on a length scale equal to the transport mean free path. In this work we hypothesized that polarization contrast could be similarly detected optoacoustically based on the preferential absorption of polarized light in tissues. It is demonstrated here by means of tissue-mimicking phantom experiments that the suggested method is capable of accurately resolving polarized structures submerged 5 mm and more into highly scattering and absorbing medium. This contrast mechanism could be efficiently used for both intrinsic imaging of tissue structures presenting polarization dependent absorption or for other applications, e.g. development of new polarization-based contrast agents.

* Electronic mail: daniel.razansky@helmholtz-muenchen.de

Photons Plus Ultrasound: Imaging and Sensing 2009, edited by Alexander A. Oraevsky, Lihong V. Wang,
Proc. of SPIE Vol. 7177, 71770M · © 2009 SPIE · CCC code: 1605-7422/09/$18 · doi: 10.1117/12.810605

II. METHODS

Schematic of optoacoustic measurement geometry is shown in Fig. 1. For excitation we used a tunable optical parametric oscillator laser (Vibrant-532-I, Opotek Inc., Carlsbad, California) with a pulse duration below 10 ns and a repetition frequency of 20 Hz. For the ultrasonic detection we used a broadband transducer with a central frequency of 3.7 MHz and 75% bandwidth (Model V382, Panametrics-NDT, Waltham, Massachusetts) cylindrically focused in the image plane. The recorded signals were amplified, digitized, and averaged by an acquisition card with 100 Msps (NI PCI-5122, National Instruments Corp., Austin, Texas) and 14 bit digital resolution.

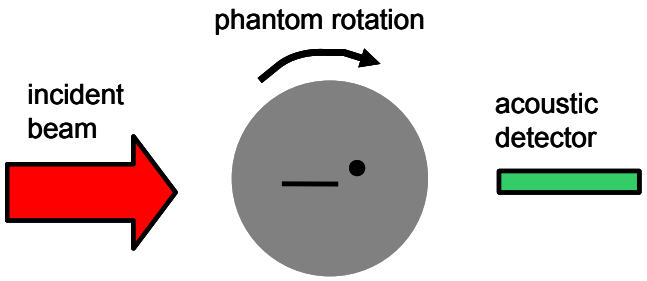

Fig. 1. Schematic top view of optoacoustic tomographic data acquisition

III. RESULTS

In the first set of experiments (Fig. 2(a)), a 0.5 mm thick polarized film was incorporated at a depth *d* within a turbid medium consisting of 3% (by volume) of Lyposin-II-10% (Hospira Inc., Lake Forest, IL), which provided reduced scattering coefficient of $\mu_s' = 2.5cm^{-1}$ [6]. The polarization direction of the input laser beam was rotated using half-wave plate and the optoacoustic signals for different polarization angles and film depths were subsequently recorded. The results for the relative intensity of the optoacoustic signals versus polarization angle and target depth are depicted in Fig. 2(b). The polarized film acts as an analyzer for the incoming laser beam with the optoacoustic signal following the Malus' law with a $\sin^2$ dependence on twice the half-wave plate angle. When the incoming beam is cross-polarized with respect to film polarization orientation, it corresponds to a minimum in transmission (maximum optoacoustic signal) through the film. Naturally, as the film depth increases, the light undergoes depolarization therefore the relative changes in optoacoustic signal due to polarization rotation are decreasing.

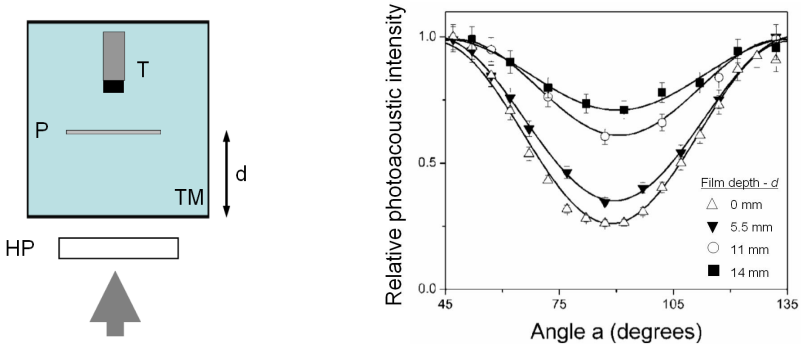

(a) (b)

Fig. 2. Optoacoustic polarization measurements. (a) Diagram of the experimental setup: HP – half-wave plate; TM- turbid medium; P –polarized film; T – transducer. (b) Relative intensity of the recorded optoacoustic response versus the angle of half-wave plate for different polarizer depths.

For comparison, we used a CCD camera (Fig. 3(a)) in order to measure depolarization of light as it passes through a turbid slab of varying thickness *d* having scattering properties similar to the previous experiment. The results are presented in Fig. 3(b) and are in good agreement with the optoacoustic measurements from Fig. 2(b), with here the signal intensity presenting the similar $\sin^2$ dependence on the half-wave plate angle

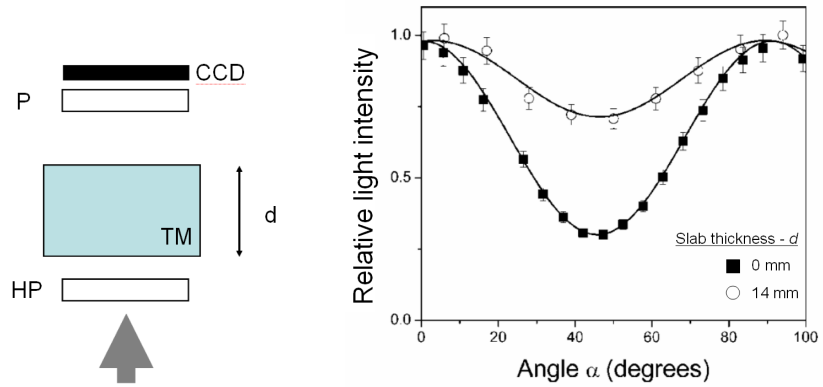

(a) (b)

Fig. 3. Optical polarization measurements. (a) Diagram of the experimental setup; (b) Relative peak intensity recorded by the CCD camera versus the angle of half-wave plate (HP) for two different thicknesses of turbid medium (TM).

Finally, we used the optoacoustic tomography setup (Fig. 1) in order to reconstruct images from a heterogeneous tissue-mimicking phantom that in addition has polarization contrast. For this, a cylindrical 10 mm diameter phantom was created by molding 0.006% (by volume) of India ink (Higgins, Sanford Bellwood, IL) and 24% of Lyposin-II-10% in agar in order to provide background optical absorption of $\mu_a = 0.3cm^{-1}$ and reduced scattering coefficient of $\mu_s^{'} = 20cm^{-1}$ at the 750 nm wavelength employed. To create polarization contrast, 3 mm wide strip of polarized film was introduced in the middle of the phantom. In addition, a cylindrical insertion having 0.8mm diameter and higher optical absorption coefficient of $\mu_a = 1cm^{-1}$ was introduced as control. The phantom was fixed on the rotation stage (Newport Corp., Irvine, CA) and rotated 360° with 3° steps to allow for two-dimensional image reconstruction using filtered back-projection. The details of the experimental setup can be found elsewhere [4,6]. Optoacoustic images for the two polarization states are presented in Fig. 4(a) and (b) and apparently attain similar appearance, providing no useful information on the actual polarization contrast of the internal structures. In contrast, the difference image (Fig. 4(c)) clearly suppresses other structures and emphasizes the polarized strip with both high contrast and high spatial resolution on the order of 150 microns, corresponding to the useful bandwidth of the ultrasonic transducer (5Mhz).

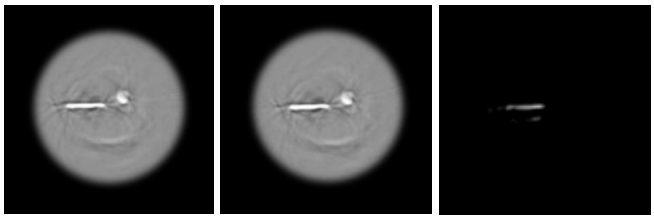

Fig. 4. Optoacoustic tomography images of a thin polarized film incorporated into heterogeneous tissue-mimicking phantom. Images for polarization angles providing maximal and minimal optoacoustic response from the film are presented in (a) and (b), respectively; (c) Difference image between (a) and (b).

IV. DISCUSSION AND CONCLUSIONS

We have presented a new mechanism of contrast for optoacoustic imaging exploiting optical polarization. The method was further shown capable of accurately resolving polarized structures embedded deep in turbid medium having tissue-like optical and acoustic properties. This contrast mechanism could be efficiently used for both intrinsic imaging of tissue structures presenting polarization dependent absorption (dichroism) or for development of new polarization-based contrast agents.

Polarization imaging has already developed many applications around morphological contrast mechanisms in surface or endoscopic tissue imaging, for example skin cancer differentiation or atherosclerotic plaque characterization [12, 13]. Polarization has also been associated with orientation effects in fluorescence molecules [14]. Since spatial resolution of optoacoustic tomography is not limited by the diffusion path length, it could propagate the *in-vivo* study of some of these phenomena deeper in tissue with superior resolution compared to the one granted by conventional optical polarization imaging.

The particular advantage of optoacoustics over other absorption-sensitive techniques, e.g. diffusion optical tomography (DOT), is its ability to resolve structures with dimensions well below diffusion path length, opening the possibility for high-resolution polarization imaging deep in turbid media. As opposed to other backward detection optical imaging modalities that record the light upon its return onto tissue surface, optoacoustics senses polarization-dependent absorption within the medium, thus can penetrate at least twice as deep while preserving high spatial resolution. Finally, the presented polarization-sensitive optoacoustic imaging method opens interesting possibilities for studies of light

depolarization in intact tissues as well as for general verification of theories of polarized light propagation in turbid media.

REFERENCES

[1] Gusev V. E., and Karabutov A. A.. 1993. *Laser Optoacoustics*, Am. Inst. Phys., New-York.

[2] Wang X., Pang Y., Ku G., Stoica G., and Wang L. V.. "Noninvasive laser-induced photoacoustic tomography for structural and functional in-vivo imaging of the brain", *Nat. Biotechnol.* 21: 803-806 (2003).

[3] Ku G., Wang X., Xie X., Stoica G., and Wang L. V., "Imaging of tumor angiogenesis in rat brains in vivo by photoacoustic tomography", *Appl. Opt*. 44: 770-775 (2005).

[4] Razansky D., Vinegoni C., and Ntziachristos V., "Multi-spectral photoacoustic imaging of fluorochromes in small animals", *Opt. Lett.* 32(19): 2891-2893 (2007).

[5] Mallidi S., Larson T., Aaron J., Sokolov K., and Emelianov S., "Molecular specific optoacoustic imaging with plasmonic nanoparticles", *Opt. Express* 15(11): 6583-6588 (2007).

[6] Razansky D, and Ntziachristos V., "Hybrid photo-acoustic fluorescence molecular tomography using finite-element-based inversion", *Med. Phys.* 34(11): 4293-4301 (2007).

[7] Wu P. J., and Walsh J. T., "Stokes polarimetry imaging of rat-tail tissue in a turbid medium: Degree of linear polarization image-maps using incident linearly polarized light", *J. Biomed. Opt.* 11(1): 014031 (2006).

[8] Kuhn J. R., Wu Z., and Poenie M., "Modulated Polarization Microscopy: A Promising New Approach to Visualizing Cytoskeletal Dynamics in Living Cells", *Biophys J.* 80: 972-985 (2001).

[9] Jin L.-W., Claborn K. A., Kurimoto M., et al, "Imaging linear birefringence and dichroism in cerebral amyloid pathologies", *PNAS* 100(26): 15294-15298 (2003).

[10] Xu M., and Alfano R. R., "Random walk of polarized light in turbid medium", *Phys. Rev. Lett.* 95: 213901 (2005).

[11] Demos S. G., Radousky H., and Alfano R., "Deep subsurface imaging in tissues using spectral and polarization filtering", *Opt. Express* 7: 23-28 (2000).

[12] Jacques S. L., Roman J. R., and Lee K., "Imaging skin pathology with polarized light", *J. Biomed. Opt*. 7(3): 329-340 (2000).

[13] Nadkarni S. K., Pierce M. C., Park B. H., et al, "Measurement of collagen and smooth muscle cell content in atherosclerotic plaques using polarization-sensitive optical coherence tomography", *J Am Coll Cardiol*. 49(13): 1474-1481 (2007).

[14] Rizzo M. A., and Piston D. W., "High-Contrast Imaging of Fluorescent Protein FRET by Fluorescence Polarization Microscopy", *Biophys J.* 88(2): L14–L16 (2005).